Supermartensitic Stainless Steel Deposits: Effects of Shielding Gas and Postweld Heat Treatment

Detailed are the results as CO_2 content in the shielding gas increased, plus the postweld heat treatment utilized in this work

BY S. ZAPPA, H. G. SVOBODA, AND E. S. SURIAN

ABSTRACT

Welding supermartensitic stainless steel plays a crucial role in structural components, influencing their toughness and resistance to sulfide stress cracking. Postweld heat treatment (PWHT) adjusts the final properties of the weldments, bearing on microstructural evolution. The objective of this work was to study the effects of different shielding gas mixtures and PWHT on supermartensitic stainless steel all-weld-metal properties. Three all-weld-metal test coupons were prepared according to standard ANSI/AWS A5.22:95, *Specification for Stainless Steel Electrodes for Flux Cored Arc Welding and Stainless Steel Flux Cored Rods for Gas Tungsten Arc Welding*, using a 1.2-mm-diameter tubular, metal-cored wire under Ar-5% He, Ar-2% CO_2, and Ar-18% CO_2 gas shielding mixtures in the flat position with a nominal heat input of 1 kJ mm^{-1}. The PWHT used was 650°C for 15 min. All-weld metal chemical composition analysis, metallurgical characterization, hardness and tensile property measurements, and Charpy V-notch tests were carried out. It was found that as CO_2 increased in the shielding gas C, O, and N contents increased as well as mechanical properties varied; hardness and ultimate tensile strength increased, and toughness decreased. The PWHT improved toughness. Technological property of the consumable was also studied.

Introduction

Over the years, 13% Cr steel has been widely accepted in the oil country tubular goods (OCTG) segment because of its good corrosion resistance. The use of 13% Cr steel is recognized as a standard countermeasure to corrosion attack initiated by carbon dioxide in oil and gas welds. However, conventional type 12–13% Cr steel has not been utilized so much in line pipe because of its relatively bad weldability, which requires preheating prior to welding and postweld heat treatment (PWHT) (Ref. 1).

Recently, supermartensitic stainless steels (SMSS) have been developed as an attractive technical alternative to high-strength, low-alloy (HSLA) steels mainly in applications related to the oil and gas industry (Refs. 2, 3). Welding these materials plays a crucial role in structural components, influencing their weldability, toughness, and resistance to sulfide stress cracking. The SMSS were developed based on classic martensitic stainless steels (11–14% Cr), reducing C content to enhance weldability, toughness, and corrosion resistance, plus adding Ni to promote a free ferrite structure and Mo (Refs. 4, 5), which also improves corrosion resistance (Refs. 6, 7).

For welding these materials, gas metal arc welding (GMAW) using SMSS metal-cored wires has been recognized as a suitable technological option, and its use has recently been improved (Ref. 5). This type of consumable presents several advantages such as low slag generation and high deposition rate (Ref. 8). Shielding gases employed for welding this type of material usually are inert gas mixes (Ar-He) or Ar-rich mixtures. The type of shielding gas can affect the chemical composition of the weld metal, principally O, N, and C contents (Ref. 9).

Usually, PWHT is necessary to adjust the properties of weldments in SMSS. In these cases, the heat treatment times typically vary between 5 and 30 min. In this respect, it has been reported that the aforementioned short PWHT provides an improvement in sulfide stress cracking (SSC) resistance (Ref. 7). In certain grades of SMSS, these treatments provide a decrease of hardness and residual stress along with increased toughness, while grades with higher Mo content are less sensitive to PWHT (Refs. 7, 10).

Different PWHTs lead to microstructural modifications producing different combinations of phases present in SMSS weld deposits (tempered and untempered martensite, austenite, carbides, etc.) with each microstructural pattern affecting toughness in a specific way.

The objective of this work was to systematically study the effects of different shielding gas mixtures and PWHT (650°C × 15 min) on the all-weld-metal properties ob-

S. ZAPPA (zappasebastian@hotmail.com) *is with the Research Secretariat, Faculty of Engineering, University of Lomas de Zamora, Buenos Aires, Argentina. H. G. SVOBODA is with the Materials and Structures Laboratory, Faculty of Engineering, Intecin, University of Buenos Aires, Conicet, Buenos Aires, Argentina. E. S. SURIAN is with the Research Secretariat, Faculty of Engineering, University of Lomas de Zamora, Buenos Aires and Deytema, Regional Faculty of San Nicolás, National Technological University, San Nicolás, Argentina.*

KEYWORDS

Supermartensitic Stainless Steel
Shielding Gas
Postweld Heat Treatment (PWHT)
Mechanical Properties

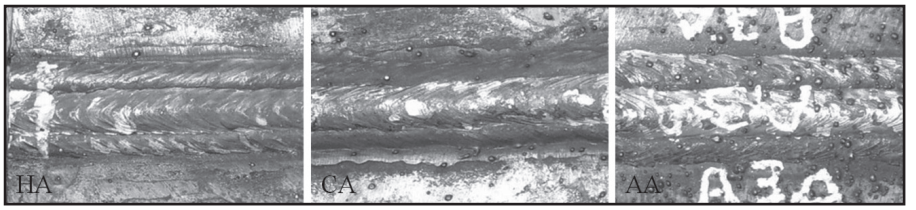

Fig. 1 — Surface appearance of welded samples for the three gases.

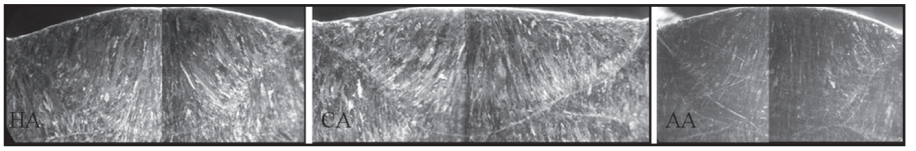

Fig. 2 — Last weld bead for the different shielding gases.

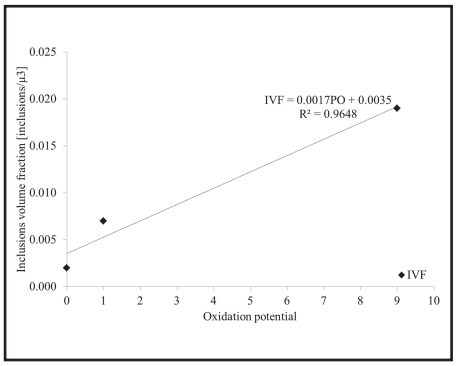

Fig. 3 — Inclusions volume fraction vs. oxidation potential of the shielding gas.

tained with a SMSS metal-cored wire used with the semiautomatic welding process.

Experimental Procedure

The oxidation potential (OP) of a shielding gas is related to O_2 and CO_2 contents of the mentioned gas, according to the following equation (Ref. 11):

$$OP = O_2 + 0.5\ CO_2$$

Table 1 shows the chemical composition of shielding gases used and their respective OP, the samples identification, and welding parameters utilized. Three all-weld-metal coupons were welded according to the standard ANSI/AWS A5.22-95, *Specification for Stainless Steel Electrodes for Flux Cored Arc Welding and Stainless Steel Flux Cored Rods for Gas Tungsten Arc Welding*, using a tubular metal-core wire of 1.2 mm diameter with three different shielding gases. In all cases, the welding position was flat, and the preheating and interpass temperatures were 100°C. Gas flow was 18 L/min and stickout 20 mm. After welding, the three coupons were X-rayed following ANSI B31.3-96, *Chemical Plant and Petroleum Refinery Piping*.

A PWHT at 650°C for 15 min was applied to the different samples in an induction heating furnace. This PWHT condition was chosen according to the recommendations of the consumable manufacturer and previous studies (Refs. 12, 13). From each welded coupon, transversal sections for macro and microstructure studies, chemical composition determination, and hardness measurements were extracted. To study the operability of the consumable, width and penetration of the last bead were measured as well as the spatter level as a function of the shielding gas used.

On the cross sections of each coupon, chemical composition by optical emission spectrometry (OES) was determined, except the C, O, N, and S contents, which were analyzed using a Leco™. The inclusionary levels and critical temperatures were determined. The microstructural characterization was performed by light microscopy (LM), scanning electron microscopy (SEM), and X-ray diffraction (XRD). The delta ferrite fraction present in each deposit was measured through quantitative metallography according to ASTM E562-99, *Standard Test Method for Determining Volume Fraction by Systematic Manual Point Count*, and the retained austenite contents were determined using a peak comparison method from the XRD patterns (Ref. 14).

In addition, Vickers hardness HV1 was measured. From each coupon, 1 longitudinal tensile specimen was machined according to (Ref. 15), and 15 Charpy V-notch (CVN) impact specimens were machined according to ASTM E23-05, *Standard Test Methods for Notched Bar Impact Testing of Metallic Materials*. Tensile and impact CVN samples were tested in the as-welded (AW) and PWHT conditions. Tensile property was measured at room temperature, and CVN impact tests were performed at 20°, 0°, –20°, –40°, and –60°C.

Results and Discussion

According to ANSI B31.3-96, all coupons were approved as they presented very low defect levels.

Figure 1 shows the surface appearance of samples HA, CA, and AA welded under each shielding gas used. It can be seen that there was a clear increase in the amount of spatter as the CO_2 content in the shielding gas increased. This could be associated with an increased partial pressure of CO_2 in the arc atmosphere.

For the welding parameters used, the metal transfer occurred in a mixed globular/spray mode. The change from a transfer mode to another one is characterized by a transition current, which depends on the shielding gas and increases with its CO_2 content. In the gas atmosphere, the presence of this gas limits the electromagnetic forces that control spray transfer mode (Ref. 16). In this sense, when using a gas mixture with higher amounts of CO_2, the globular to spray transfer mode transition current increases, then increasing the level of spatter associated with the globular transfer mode.

Figure 2 shows the images of the last bead for HA, CA, and AA specimens. In these figures, it can be seen that as CO_2 content increased in the shielding gas, the geometry of the bead changed, decreasing the ratio width/penetration as is shown in Table 2.

Table 1 — Chemical Composition of Shielding Gases Used, Samples Identification and Welding Parameters

As Welded	Heat Treated	Shielding Gas	CO_2 (%)	Ar (%)	He (%)	OP	Tension (V)	Current (A)	Welding Rate (mm/s)	Heat Input (kJ/mm)
HA	HP	Ar + 5% He	0	70	5	0	25	226	5	1.1
CA	CP	Ar + 2% CO_2	2	98	0	1	25	230	6	1.0
AA	AP	Ar + 18% CO_2	18	82	0	9	26	232	6	1.0

Table 3 shows the results of the chemical composition of all-weld-metal coupons. Carbon contents, fluctuating between 140 and 180 ppm, were higher than expected for this consumable. The value reported by the manufacturer was less than 100 ppm (Refs. 13, 17).

In general, the measured values of the rest of the analyzed elements were below the nominal values with the exception of Si and Mo, according to the product data sheet (Ref. 13). In the SMSS, to achieve good toughness and appropriate hardness values, it is necessary to have low C, N, O, and S contents (Refs. 18, 19). The C content controls the martensite hardness and toughness; it is the more influential element on M_S temperature. The precipitated carbides influence corrosion resistance and hydrogen damage (Ref. 20), among others. Also, the presence of N and Mo has a great influence on the sequence of carbides and carbides/nitrides precipitation (Ref. 21).

Regarding the O content present in the weld metal, in all cases it exceeded 300 ppm, the limit beyond which, according to the literature (Ref. 17), the absorbed energy falls brusquely. The variation observed in the chemical composition of the all-weld metal corresponds, among other things, to the metallic elements oxidation process occurring in the electric arc. The greater O content in the shielding gas, the higher oxidation potential of the gaseous atmosphere, and the greater the effect of oxidation mentioned above (Ref. 22). The high interstitial elements contents in the deposits are associated with a high content of O and C in the atmosphere of the arc from the decomposition of CO_2 in the shielding gas (Ref. 23). These variations were small but could have affected certain properties. In this sense, Ni, Cu, and Mn are elements that stabilize the austenite, so that higher contents of these elements could result in an increase of retained austenite in the microstructure (Refs. 16, 24).

Also, Mo and Cr could affect the delta ferrite fraction as they both stabilize this phase. Toughness and, to a lesser extent, tensile property and corrosion resistance, could be affected by these small variations in chemical composition, mainly in the coupons welded under a high OP gas mixture.

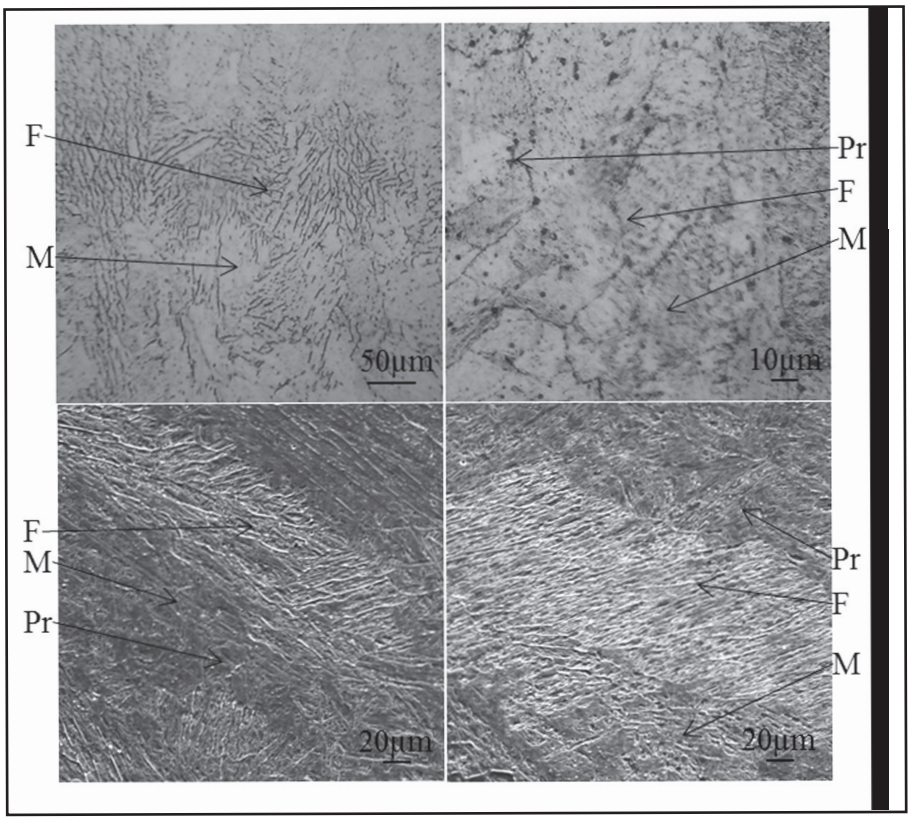

Fig. 4 — LM and SEM in the coupon AP.

The increase of CO_2 content in the shielding gas produced a higher O content in the deposits. One way to demonstrate the increase of this last element is through the determination of inclusionary levels. Some authors (Ref. 25) reported that the sizes of the inclusions are the order of microns. Table 4 shows that quantity, average diameter, and volume fraction of inclusions in the AW sample increased with the CO_2 content in the shielding gas.

Figure 3 presents the effect of the shielding gas on the inclusion volume fraction (IVF) of the deposits, showing the tendency mentioned. These differences in the inclusionary level may affect, among other properties, the toughness and corrosion resistance of the deposits (Refs. 17, 18, 25, 26).

In all cases, in the AW samples, the microstructure consisted of a martensitic matrix with small amounts of delta ferrite and retained austenite. The literature (Refs. 6, 7, 27) reports for this type of steel that retained austenite contents in the AW condition may vary between 2 and 30%, and that this phase cannot be identified through the microscopy techniques used in this work (Refs. 12, 17, 26). Samples submitted to PWHT presented a darkening of the martensitic structure associated with the carbide and/or carbonitride precipitates mainly in the grain boundary.

Table 2 — Relationships Width/Penetration for the HA, CA, and AA Samples

Sample	Relationship Width/Penetration
HA	2.7
CA	2.2
AA	1.9

Table 3 — Chemical Composition

Sample	C (ppm)	Mn (%)	Si (%)	S (%)	Cr (%)	Ni (%)	Mo (%)	Cu (%)	V (%)	O (ppm)	N (ppm)
HA	140	1.72	0.44	0.015	11.8	6.2	2.69	0.48	0.09	380	50
CA	150	1.75	0.45	0.014	11.7	6.2	2.66	0.48	0.09	440	60
AA	180	1.57	0.42	0.016	11.7	6.1	2.47	0.41	0.09	710	140
Specif.	<100	1.8	0.4	NI	12.5	6.7	2.5	0.5	NI	NI	<100

NI: not informed

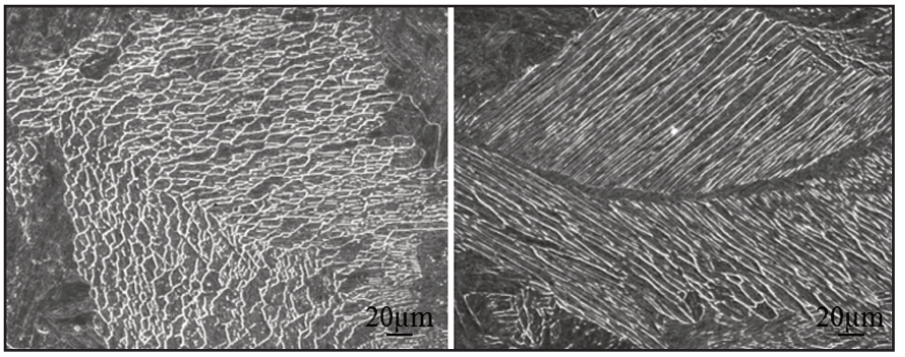

Fig. 5 — Different morphologies of ferrite in the HA coupon.

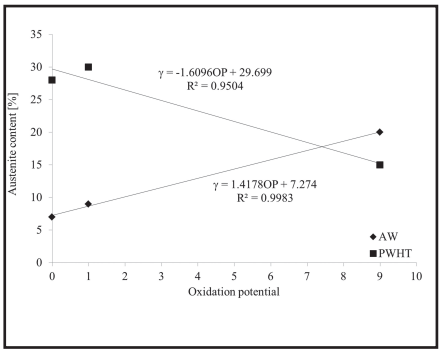

Fig. 6 — Relationship between the austenite content and oxidation potential of the shielding gas.

Table 4 — Inclusionary Analysis

Sample	IT	Area (μm^2)	ID (incl/ μm^2)	IAD (μm)	IVF (incl/μm^3)	OP	O Content
HA	5	1695	0.003	1.14	0.002	0	380
CA	14	1695	0.008	1.26	0.007	1	440
AA	32	1695	0.019	1.40	0.019	9	710

IT: inclusions total; ID: inclusions density; IAD: inclusions average diameter; IVF: inclusions volume fraction; OP (oxygen potential) = O_2 + 0.5 CO_2

Figure 4 shows the microstructure of the coupon AP obtained by LM and SEM, respectively. In this figure the following identification was used: M, martensite; F, ferrite; and Pr, precipitates. Similar microstructures were found in the rest of the coupons.

In the literature (Ref. 17), there are reported several ferrite morphologies found in SMSS deposits. Two types of ferrite could be identified based on their location and morphology. Most common was ferrite with morphology very similar to that of ferrite found in duplex stainless steel weld metals. The presence of this ferrite is a consequence of incomplete ferrite-to-austenite transformation in weld metals solidifying as ferrite and was most common for more highly alloyed weld metals (Ref. 17). Another ferrite morphology, similar to that seen in austenitic stainless steel weld metals, was found in weld metals higher in Ni, solidifying as a mixture of ferrite and austenite (Ref. 17). This ferrite was located in the last solidifying interdendritic regions.

Figure 5 shows the different ferrite morphology for the HA coupon. These different morphologies of ferrite in the microstructure show different solidification modes generated simultaneously in the deposits.

The critical temperatures A_{C1}, A_{C3}, and M_S were determined by dilatometry with a heating rate of 1°C/min in the HA and AA coupons. Table 5 shows the results obtained. The coupon welded with high CO_2 content in the shielding gas (AA) had a higher austenite transformation starting temperature regarding the coupon welded under Ar + 5% He (HA). Marshall and Farrar (Ref. 28) indicated that the actual A_{C1} temperature for a low-grade stainless steel is around 650°C while high-grade alloys are around 630°C.

The use of equations for the selection of PWHT temperature should be carefully considered and the results be verified experimentally to prevent undesired hardening of the structure due to the fact that partial austenitizing can generate fresh martensite (Ref. 5). The PWHT is usually recommended in SMSS deposits for improving both toughness and ductility; tensile strength is reduced by only 10 to 20% (Ref. 29). Ni has a strong effect on decreasing A_{C1} and Mo the contrary effect. In this sense, the small variations of certain elements observed in the chemical composition of these samples could have led to changes in critical temperatures.

The different types of ferrite were quantified for the three coupons in AW conditions through 20 measurements on a grid of 660 points. Table 6 shows these results. There were no significant variations in the measured ferrite contents, indicating no shielding gas important influence on these values. Table 7 shows the retained austenite content.

From a microstructural point of view, the objective of PWHT is to temper the martensite and increase the stable retained austenite at room temperature resulting in softening and improving both toughness and corrosion resistance of the deposit (Refs. 2, 3, 19, 30, 31). The literature reports (Refs. 5, 32) that a PWHT at 650°C for 5 min is the heat treatment commonly used in manufacturing SMSS pipe when using duplex and superduplex stainless steel consumables; longer heat treatment can cause sigma phase to form in these weld metals. During the PWHT, in these steels, the tempering of martensite is generally followed by a softening associated with incoherent carbide precipitation, achieving the maximum softening with the $M_{23}C_6$ carbide precipitation at about 500°C (Ref. 32).

In alloys without Ni, the PWHT is performed at about 700°C to obtain a high reaction rate and maximum softening (Ref. 32). The presence of Ni reduces the critical transformation temperature A_{C1}. This temperature, for a given steel, depends on the chemical composition, heating rate, and in alloys with high Ni contents can be as low as 500°–550°C (Refs. 32, 33). In this work, heat treatment was carried out at 650°C for 15 min, which seemed to be adequate for matching filler metals but not appropriate for duplex or superduplex ones. This temperature/time parameter did not generate changes that could have been observed by LM and SEM. Only differences in the austenite content in the microstructure could be established by X-ray diffraction.

As mentioned above, in alloys with high contents of Ni, the A_{C1} temperature may be around 550°C. At this temperature, the kinetics of carbide formation is very slow and, it is normal that austenite precipitates (Ref. 32). In this way, through a diffusion mechanism, the austenite formed during PWHT will have a different chemical composition from the austenite retained during the welding process (Refs. 32, 34). In this instance, the martensitic matrix and retained austenite produced during welding will have identical chemical composition while the new austenite formed during PWHT will be

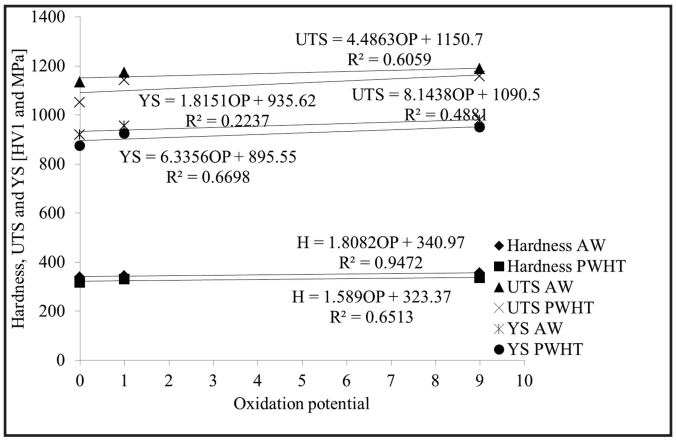

Fig. 7 — Influence of OP on hardness, ultimate tensile, and yield strengths.

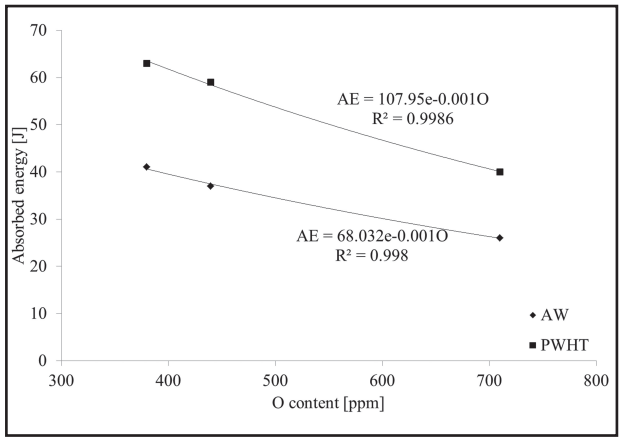

Fig. 8 — Effect of O content on the CVN absorbed energy in AW and PWHT conditions.

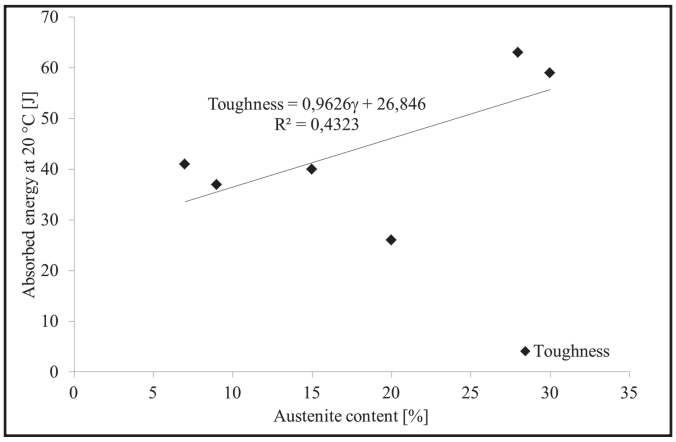

Fig. 9 — The CVN at 20°C vs. austenite content.

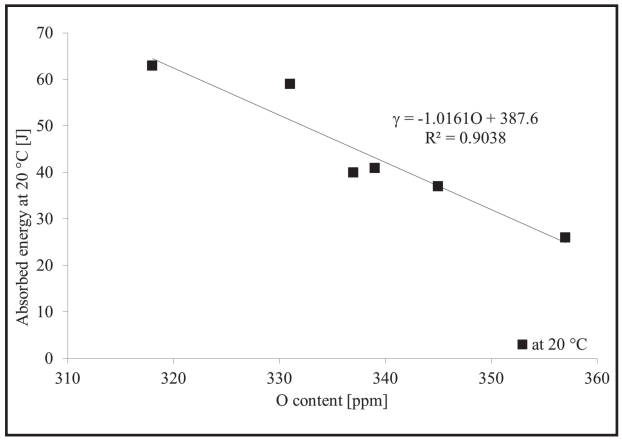

Fig. 10 — Hardness vs. CVN in AW and PWHT conditions at 20°C.

richer in N, C, and Ni. This degree of enrichment determines the stability of austenite formed during the heat treatment.

If PWHT is performed at temperatures slightly above A_{C1}, the enriched austenite is stable at room temperature (Refs. 32, 34). If PWHT is carried out at temperatures well above A_{C1}, the austenite formed during PWHT will be transformed to "fresh" martensite during cooling (Ref. 32). If PWHT is carried out below A_{C1} temperature, the austenite content will decrease with respect to that of the AW sample because part of it will transform to "fresh" martensite after cooling to room temperature.

Figure 6 shows the relationship between austenite content and OP of the shielding gas for both AW and PWHT conditions. The contents of retained austenite increased with increasing CO_2 in the shielding gas in AW samples. This increase could be related to higher C and N content generated using higher amounts of CO_2 in the shielding gas as both elements are strong promoters of austenite.

Also, it has been reported (Ref. 35) that the austenite contents are strongly controlled by the M_S temperature. Retained austenite levels, at room temperature, are higher when M_S decreases (Ref. 35). As seen previously, increasing the OP in the shielding gas slightly decreased the transformation temperature of austenite to martensite during cooling. This slight decrease in the M_S temperature generated a higher retained austenite content at room temperature, in accord with what was reported elsewhere (Ref. 35).

When applying PWHT, retained austenite content increased for low OP, while for high OP retained austenite values decreased. The higher OP, the higher critical temperature measured. The HA coupon (A_{C1} = 590°C) showed low austenite values in the AW condition and application of PWHT, at a temperature slightly above A_{C1}, then generated higher amounts of retained austenite. On the other hand, the AA coupon (A_{C1} = 660°C) had a higher content of austenite in the AW condition and applying PWHT, which was slightly below the critical temperature, generated lower retained austenite content regarding the AW sample. In conclusion, applying a PWHT at 650°C for 15 min to this type of material, austenite content can decrease or increase depending on the PWHT temperature location regarding the A_{C1} critical temperature of the material.

Table 8 presents the values of hardness, tension property, and toughness deter-

Table 5 — Critical Temperatures for Samples H and A

Sample	Heating Rate (°C/min)	A_{C1} (°C)	A_{C3} (°C)	MS (°C)
HA	1	590	670	125
AA	1	660	710	115

Table 6 — Ferrite Content

Sample	HA	CA	AA
Ferrite Measured (%)	8.5	10.8	9.3

Table 7 — Retained Austenite

Sample	HA	CA	AA	HP	CP	AP
Retained Austenite Measured (%)	7	9	20	28	30	15

Table 8 — Mechanical Properties

Sample	Hardness (H_{V1})	UTS (MPa)	YS (MPa)	E (%)	AR (%)	CVN (J)/(°C) 20	0	–20	–40	–60
HA	339	1134	920	17	45	41	33	31	29	28
CA	345	1174	955	15	40	37	36	34	33	32
AA	357	1189	980	12	33	26	24	21	19	18
HP	318	1052	875	19	53	63	51	45	43	43
CP	331	1142	925	15	40	59	48	45	43	38
AP	337	1159	950	13	37	40	35	34	32	32

UTS: ultimate tensile strength; YS: yield strength; E: elongation to fracture; AR: area reduction

mined on the all-weld-metal coupon for the different conditions studied. Figure 7 shows the influence of OP on hardness, ultimate tensile strength, and yield strength for the AW and PWHT samples. It can be seen that as the gas OP increased, hardness increased; this fact can be related to the augmentation of C and N in the deposits as the OP increased (Ref. 18).

It is known (Refs. 36–38) that C content controls the martensite hardness. The higher C content the higher measured hardness. The literature also reports (Refs. 39, 40) that N is a promoter of carbonitrides that generates a hardening of the structure in these materials. Then, higher both C and N contents will produce higher hardness. The tensile and yield strengths showed the same behavior that hardness did. The application of PWHT resulted in lower values of hardness, tensile strength, and yield strength in all cases. As mentioned above, the PWHT employed generated martensite tempering and in some cases higher austenite content at room temperature; these two facts produced lower values of mechanical properties.

It was not possible to establish a relationship between austenite contents and the tensile properties and hardness. The absorbed energy values obtained were in the order of these reported in the literature (Refs. 17, 37, 41, 42). In the AW samples, the biggest value was achieved in sample HA (no CO_2 in the shielding gas) with 41 J at 20°C. The effect of OP on the toughness of these materials was clearly seen: The higher CO_2 in the shielding gas, the lower toughness for both AW and heat-treated samples. According to the literature (Ref. 17), O content strongly influences the toughness values of the SMSS.

Figure 8 shows the relationship between toughness results at 20°C and the O content in all welded metal coupon in both AW and PWHT samples. This figure shows clearly that the toughness decreased when the O content increased for all coupons. The same trends could be determined for all test temperature. In all cases, the absorbed energy values achieved after PWHT improved for all temperatures, resulting over 50% higher to those obtained in AW samples. The PWHT applied, as discussed above, produced martensite tempering and, according to the location of PWHT temperature with respect to A_{C1} temperature, generated lower or higher austenite content in the microstructure (Ref. 43) regarding the microstructure in AW condition. The microstructure of PWHT samples consisted of tempered martensite, delta ferrite, and austenite fractions.

It is known (Ref. 43) that higher stable austenite content at room temperature increases the absorbed energy in the CVN impact test. It was not possible to establish a direct relationship between austenite content and toughness. However, according to Fig. 9, it can be seen that as the austenite content increased, toughness tended to increase. A low R^2 could be indicating that austenite content is not the only factor influencing toughness.

Figure 10 shows the relationship between the hardness and toughness in AW and PWHT conditions at 20°C.

Conclusions

As CO_2 content in the shielding gas increased, the following occurred:

1) Higher spatter and a lower width-penetration relationship in the last bead were obtained.

2) In the all-weld metal, C, O, and N contents increased. Mn, Si, Cr, Ni, and Mo contents decreased.

3) Inclusionary levels increased.

4) The microstructure, in all cases, was constituted by a martensitic matrix with delta ferrite and retained austenite. The austenite content increased.

5) Hardness and tensile property slightly augmented.

6) Toughness decreased.

Regarding the PWHT used in this work, the following took place:

1) The microstructure did not show differences with the PWHT.

2) Hardness and tensile properties decreased slightly in comparison to the AW values.

3) Toughness was improved in all samples. In most cases, the absorbed energy increased in more than 50% compared to the AW samples.

4) The best toughness was achieved for those samples welded under inert gas protection and submitted to heat treatment.

In those cases where toughness is not a requirement, it is possible to use CO_2 gas shielding, especially lower cost Ar/20 CO_2.

Acknowledgments

The authors wish to express their gratitude to ESAB-Sweden for the consumable donation and Leco chemical analysis; Conarco-ESAB Argentina for performing chemical analysis; Air Liquide Argentina for donating welding gases; the Latin American Welding Foundation, Argentina, for welding and mechanical testing facilities; the Scanning Electron Microscopy Laboratory of Inti-Mechanics, Argentina, for SEM analysis facilities; and APUEMFI, Argentina, along with ANPCyT, Argentina, for financial support.

References

1. Kondo, K., et al. 1999. Alloy design of super 13Cr martensitic stainless steel (development of super 13 Cr martensitic SS for line pipe-1). *Supermartensitic Stainless Steel '99*. Brussels, Belgium.

2. Marshall, A. W., and Farrar, J. C. M. 1998. Welding of ferritic and martensitic 13% Cr steels. Preliminary report (draft 2). *IIW Doc IX-H-422-98*: 1–18.

3. Farrar, J. C., and Marshall, A. W. 1998. Supermartensitic stainless steel — Overview and weldability. *IIW Doc No. IX-H 423-98*: 1–3.

4. Bilmes, P. D. 2000. Role of austenite on the mechanical properties of soft martensitic stainless steels weld metals. PhD thesis. National University of La Plata, Faculty of Engineering. La Plata, Argentina: 147.

5. Lippold, J. C., and Kotecki, D. J. 2005.

Welding Metallurgy and Weldability of Stainless steels. John Wiley & Sons, Inc.: 1–356.

6. Karlsson, L., et al. 1999. Development of matching composition supermartensitic stainless steel welding consumables. *Svetsaren* No. 3: 3–7.

7. Kvaale, P. E., and Olsen, S. 1999. Experience with supermartensitic stainless steels in flowline applications. *Stainless Steel World*. The Hague, The Netherlands.

8. Lyttle, K., et al. 1996. Metal cored wires: Where do they fit in your future? *Welding Journal* 74(10): 35–38.

9. Zappa, S., et al. 2006. Effect of shielding gas on supermartensitic stainless steel all weld metal properties. *CONAMET/SAM*. Santiago de Chile, Chile.

10. Karlsson, L., et al. 1999. Matching composition supermartensitic stainless steel welding consumables. *Supermartensitic Stainless Steel '99*. Brussels, Belgium.

11. Stembacka, N. 1990. The influence of shielding gas on cored wires. *Welding Journal* 69(11): 43–45.

12. Zappa, S., et al. 2007. Effect of post-weld heat treatment on supermartensitic stainless steel properties deposited with e tubular metal-cored wire. *Soldagem & Inspecao* 12(2): 115–123.

13. Technical Sheet OK Tubrod, 15-55. 2004. ESAB.

14. Cullity, B. D., and Stock, S. R. 2001. *Elements of X ray Diffraction*. Prentice-Hall, 3rd Edition, New Jersey.

15. Schnadt, H. M., and Leinhard, E. W. 1963. Experimental investigation of the sharp-notch behavior of 60 steels at different temperature and strain rates. IIW-IIS Doc. 196-343-63.

16. Lancaster, J. F. 1987. *Metallurgy of Welding*. Allen & Unwin, 4th ed.

17. Karlsson, L., et al. 1999. Matching composition supermartensitic stainless steel welding consumables. *Supermartensitic Stainless Steels '99*. Brussels, Belgium.

18. Karlsson, L., et al. 2001. Mechanical properties and aging response of supermartensitic weld metals. *Stainless Steel World*. The Hague, The Netherlands.

19. Karlsson, L., et al. 2002. Welding of supermartensitic stainless steels. Recent developments and application experience. *Svetsaren*, No. 2: 15–22.

20. Zappa, S., et al. 2008. Properties, microstructure and corrosion resistance of supermartensitic stainless steel all weld metal. *CONAMET/SAM*. Santiago de Chile, Chile.

21. Pickering, F. B. 1978. *Physical Metallurgy and the Design of Steels*. Applied Science Publishers. London.

22. Vaidya, V. 2002. Shielding gas mixtures for semiautomatic welds. *Welding Journal* 81(9): 43–48.

23. Stembacka, N., and Persson, K. A. 1989. Shielding gases for gas metal arc welding. *Welding Journal* 68(11): 41–47.

24. Lippold, J., and Alexandrov, B. 2004. Phase transformation during welding and post-weld heat treatment of a 12Cr-6.5Ni-2.5Mo supermartensitic stainless steel. *Stainless Steel World*. Houston, Tex.

25. Kimura, M., et al. 2003. Mechanical properties and corrosion resistance of matching GMA welded joint for martensitic stainless steel line pipe. *Corrosion 2003*, NACE, Houston. Paper No. 03100: 1–10.

26. Karlsson, L., et al. 1999. Efficient welding of supermartensitic stainless steels with matching composition consumables. *Stainless Steel World*. The Hague, The Netherlands.

27. Zappa, S., et al. 2007. Effect of postweld heat treatment on supermartensitic stainless steel all weld metal toughness. *SAM/CONAMET*. San Nicolas, Argentina.

28. Marshall, A. W., and Farrar, J. C. M. 2001. Welding of ferritic and martensitic 11–14% Cr steels. *Welding in the World* 45 (5/6): 32–55.

29. Surian, E., et al. 2010. Welding procedure effect on SMSS all weld-metal properties. FABTECH. AWS ed. Atlanta, Ga.

30. Bilmes, P. D., et al. 2006. Microstructure and pitting corrosion of 13CrNiMo weld metals. *Corrosion Science* 48: 3261–3270.

31. Bilmes, P. D., Llorente, C. L., and Solari, M. 1998. Effect of postweld heat treatment on the microstructure and mechanical behavior of 13Cr-4NiMoL and 13Cr-6NiMoL weld metals. *The 18th ASM Heat Treating Society Conference and Exposition*. Chicago, Ill.

32. Gooch, T. G., Wolling, P., and Haynes, A. G. 1999. Welding metallurgy of low carbon 13% chromium martensitic steels. *Supermartensitic Stainless Steel*. Brussels, Belgium.

33. Arwidson, S., Baggastrom, G., and Hellner, L. 1968. New steels for the power industry. *Proc. Conf. Stainless Steels*. Birmingham: ISI publication, 117.

34. Folkhard, H. 1988. Welding metallurgy of stainless steels. *Springer-Verlag Wien*: 1–280. New York.

35. Wu, W., et al. 2000. The relationship between alloying elements and retained austenite in martensitic stainless steel welds. *Scripta Materiala* 42: 1071–1076.

36. Ramirez, J. E. 2007. Weldability evaluation of supermartensitic stainless steels. *Welding Journal* 86(5): 125-s to 134-s.

37. Perteneder, E., and Tosch, J. 1999. Important metallurgical aspects in the manual welding of soft martensitic 13% chrome steels. Brussels, Belgium.

38. Deleu, E., Dhooge, A., and Dufrane, J. J. 1999. Weldability and hot deformability of different supermartensitic stainless steel grades by weld simulation testing. *Supermartensitic Stainless Steels '99*. Brussels, Belgium.

39. Bilmes, P. D., Solari, M., and Llorente, C. L. 2001. Characteristics and effect of austenite resulting from tempering of 13Cr-NiMo martensitic steel weld metals. *Materials Characterization* 46: 285–296.

40. Bilmes, P. D., Llorente, C. L., and Solari, M. 2000. Role of the retained austenite on the mechanical properties of 13Cr-4NiMo weld metals. *The 20th ASM Heat Treating Society*. America's Center, St. Louis, Mo.

41. Heuser, H., et al. 1999. GMAW and SAW matching filler metals for supermartensitic stainless steels. *Supermartensitic Stainless Steel '99*. Brussels, Belgium.

42. Bonnel, J .M., and Butter, D. J. 1999. Supermartensitic 13% Cr stainless steel welding consumables for girth welding line pipe. *Supermartensitic Stainless Steels '99*. Brussels, Belgium.

43. Zappa, S., et al. 2008. Effect of PWHT on supermartensitic stainless steel all weld metal toughness. *Trends in Welding Research Proceedings of the 8th International Conference*. Pine Mountain, Ga.